Position of K Atoms in Doped Single-Walled Carbon Nanotube Crystals

Guanghua Gao, Tahir Çağin, and William A. Goddard III*

Materials and Process Simulation Center, Beckman Institute (139-74), Division of Chemistry and Chemical Engineering, California Institute of Technology, Pasadena, California 91125

(Received 18 November 1997)

Recent experiments by Lee *et al.* [Nature (London) **363**, 255 (1997)] show that doping carbon single-wall nanotube (SWNT) ropes with K, Rb, or Br_2 leads to metallic conductivity, but the structure and properties are not known. We used molecular dynamics to predict structures and properties which should help motivate and interpret experiments on SWNT/K. We find the optimum stoichiometry to be KC_{16} if the K cannot penetrate the tubes and K_1C_{10} ($K_5^{exo}K_3^{endo}C_{80}$, 3 within the tube) if they can. We predict the optimum structure and the associated powder-diffraction x-ray pattern expected for K_nC_{80} from $n = 0-10$ (optimum is $n = 5$). The Young's modulus per tube along the tube axis varies from 640 to 525 GPa for $n = 0$ to 5. [S0031-9007(98)06340-6]

PACS numbers: 61.48.+c, 71.15.Pd

The development of methods [1] to control the catalytic synthesis of single-wall nanotubes (SWNT's) (originally synthesized by Bethune *et al.* [2] and by Iijima [3]) to form ordered ropes containing hundreds to thousands of tubes gives hope for developing structures useful for new generations of nanoscale devices. The recent report that these SWNT ropes can be doped to form metallic conductors [4,5] gives further hope for interesting devices. Because many standard analysis techniques are difficult in the nanoscale region (10 to 100 nm), it is important to have accurate computer simulations of the structures and properties that can be correlated with observable signatures. We report methods and results that should be useful for characterizing doped SWNT.

We started with the predicted minimized crystal structure for SWNT crystals (trigonal with $a = b = 16.7$ A, $c = 4.94$ A, $\gamma = 60°$, tube-tube spacing of 16.7 A). Considering the armchair (10,10) SWNT, we allowed up to six independent SWNT per unit cell and distributed appropriate numbers of K atoms in various ways. We then carried out 20 ps of molecular dynamics (MD) to equilibrate the system and quenched the structures by minimizing the energy. We then analyzed each case to see if the pattern of K binding sites would suggest new structures to build and minimize. In these studies, we considered both trigonal (closest packed tubes) and square packing of the tubes. For trigonal crystals with n up to 2, the K intercalate between three tubes, leading to essentially the same spacing as in pristine SWNT. For $n = 3$ to 10, the K intercalate between two tubes after a sharp rise at $n = 3$, leading to 9.4% larger spacing than for pristine SWNT at $n = 10$.

In these calculations, we employed the force fields developed and used for studying the K-intercalated fullerenes [6]. We assumed that the K are fully ionized to K^+ and that the charges on the SWNT are distributed uniformly. This assumption is consistent with the assumptions used in the derivation of van der Waals parameters for *C*, *K*, and *C-K* in Ref. [6] which gave accurate results for lattice parameters and other properties for K-intercalated graphite intercalation compounds (GICs), (KC_8 and KC_{24}) and K_3C_{60}. There is still a debate in the literature as to the extent of charge transfer in GICs [7]. However, the evidence is that there is full electron transfer for stage II K-intercalated graphite, KC_{24}. On the other hand, there may not be full electron transfer for stage I K-intercalated graphite, KC_8. Considering that the diameter of the nanotubes are 1.3 nm with substantial free volume for nanotube intercalation, the *K*-doped single-walled nanotube case should be close to stage II.

Figure 1 shows the energy per carbon atom as a function of the number of intercalated K ions for two different packing schemes (square and triangular) and different doping types [exo (K atoms are allowed only in between tubes) and endo (K atoms are allowed to be inside tubes)]. Here we see that the global minimum is the trigonal structure for $K_5C_{80} = KC_{16}$. The structure projected

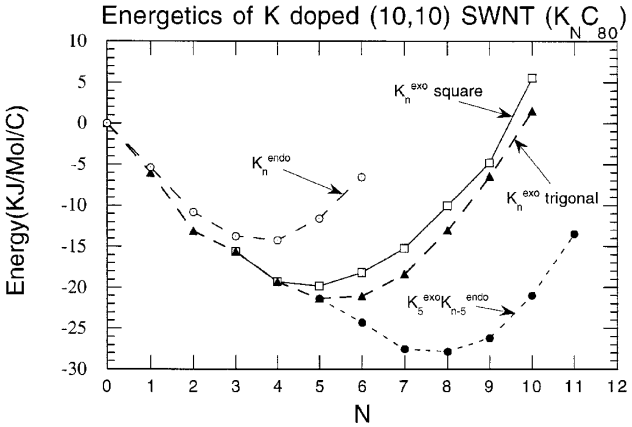

FIG. 1. The total energy per C atom for trigonal (closest packed tubes) and square packing of the tubes. For exo K, the global minimum is the trigonal structure $K_5^{exo}C_{80} = KC_{16}$. The square lattice was unstable for K_nC_{80} with $n \leq 2$.

 0031-9007/98/80(25)/5556(4)$15.00

along the c axis is shown in Fig. 2 for various cases. For $n \leq 2$ the K intercalate in hollows between three tubes, whereas for $n \geq 3$ the K intercalate between pairs of tubes, just as in intercalated graphite. Indeed Fig. 3(a) shows that for the optimum structure, $K_5C_{80} = KC_{16}$, the K are packed in the same (2×2) pattern observed for intercalated graphite, KC_8 [8]. The difference for KC_{16} SWNT is that the K can only be on the outside of the tube (*vide infra*), leading to half the amount of K. For $n \geq 7$ there are significant distortions of the tube shells.

We used quantum mechanical (QM) calculations to establish the energy of nanotubes as a function of net charge. This is required to obtain absolute energies for comparing the stability of K_nC_{80} as a function of n. The molecular mechanics (MM) and MD calculations [9] exclude Coulomb and van der Waals interactions between atoms that are bonded (1-2 interactions) or share a bonded atom (1-3 interactions). To estimate the relative energy of the SWNT with differing amounts of charge, we must include the effect of shielded 1-2 and 1-3 interactions. To do this we started with the QM [10] absolute energy of C_{60}^{q-} fullerene for $q = 0$, 1, 2, and 3 and compared this to the standard MM or MD energy for each q but with a correction term of the form $E = E_0 + \lambda Q + JQ^2$, where $Q = q/60$. We found that $\lambda = 98.737$ kJ/mol and $J = 1091.943$ kJ/mol lead to total energy differences that match the QM. These constants, λ and J, were then used for the SWNT/K calculations to obtain absolute energies.

We have not yet examined the dynamics for K diffusing through the SWNT to form the equilibrium structure. However, these results suggest a qualitative picture. The K fit quite nicely into the threefold hollows of the triangular cell, requiring no change in the tube packing up to $K_2C_{80} = KC_{40}$. Probably this diffusion is relatively rapid. Adding further K to form triangular K_3C_{80} requires a 33% volume expansion of the tubes, which could be a rather sluggish transformation. Since square K_3C_{80} and K_4C_{80} are nearly as stable as trigonal, it may be that adding K to trigonal K_2C_{80} leads to a transformation into the square phases for $n = 3, 4$. In any case, for K_5C_{80} and beyond,

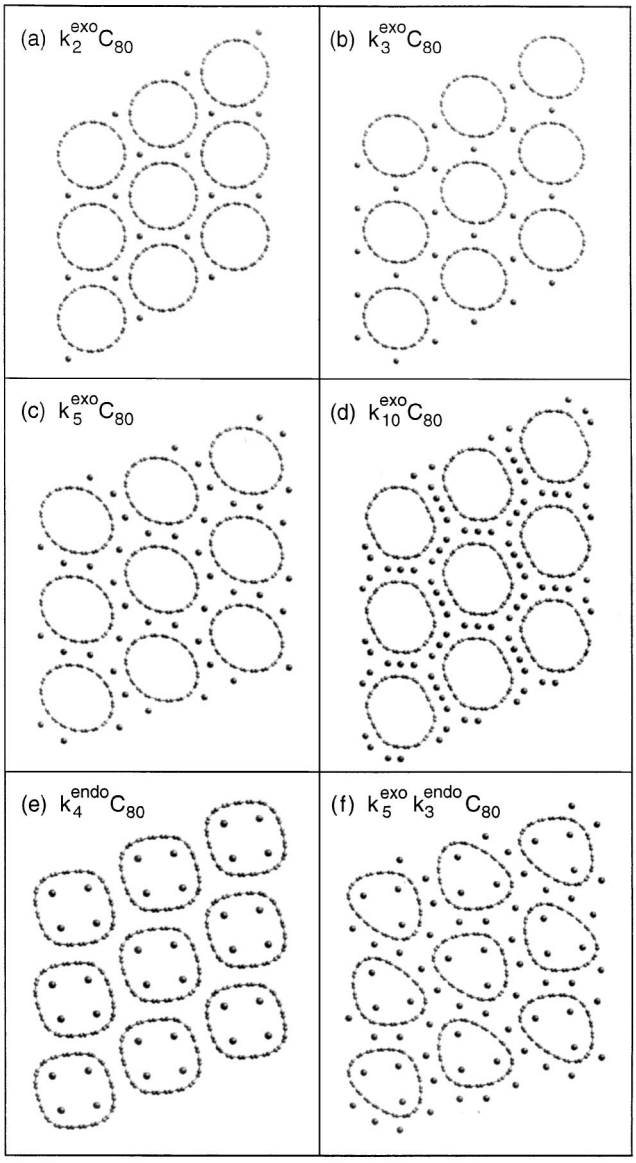

FIG. 2. The calculated optimum structures projected along the c axis for various stoichiometry and types of intercalation. For $n \leq 2$, the K^{exo} intercalate in hollows between three tubes, whereas for $n \geq 3$ the K^{exo} intercalate between pairs of tubes, just as in intercalated graphite.

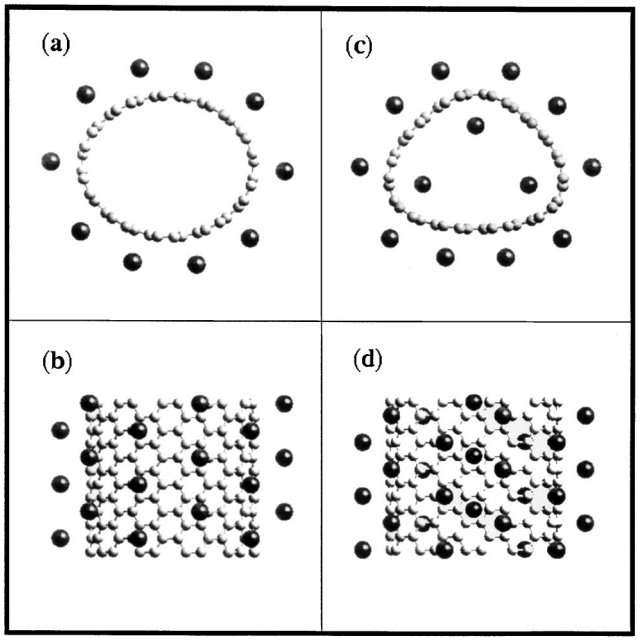

FIG. 3. (a) Top view of the $K_5^{exo}C_{80}$ triangular structure. (b) Side view of the $K_5^{exo}C_{80}$ structure. Shown is the front half of one tube plus the K associated with this surface unrolling the tube into a plane; the K exhibit the 2×2 pattern of K_5C_8 intercalated graphite. (c) Top view showing the endo K of $K_5^{exo}K_3^{endo}C_{80}$. (d) Side view of $K_5^{exo}K_3^{endo}C_{80}$.

the trigonal is strongly favored over square. Thus, we expect only the expanded triangular structure in this region.

In order to help experimentalists search for such possible interesting changes in structure, we calculated the powder diffraction and fiber diffraction patterns for all n from 0 to 10 for both square and trigonal cases. Selected cases are shown in Fig. 4.

The density and modulus along the tube axis are plotted in Fig. 5(a) as a function of n (for the trigonal case). Here, we see a dramatic break between $n = 2$ and $n = 3$ corresponding to the change in K intercalation. For $n < 2$ the K atoms are in the hollow area surrounded by three tubes, of the SWNTs [Fig. 2(a)], without distorting the circular cross section of SWNTs. However, at $n = 3$, the optimal positions of K atoms are in the midpoints of the center-to-center lines between pairs of tubes with limited distortion to circular cross sections [Fig. 2(b)]. This leads to a sharp increase in the volume 33% with respect to pristine SWNTs. (Since the c axis remains constant, this rise is due mainly to the change in the area.) As doping increased from $n = 4$ to $n = 10$ the volume (area) decreases accompanied by an increasing distortion of the SWNT shells [Figs. 2(c) and 2(d)]. The spacing between the tubes remain almost the same, approximately 10% larger than the pristine SWNT case. The Young's modulus [Fig. 5(b)] is 30% smaller for $n \geq 3$ than for $n < 3$. This is because of the change in area per tube. Normalizing by the number of tubes leads to little change in the modulus. Indeed [1090 GPa per (10,10) armchair] when normalized by the area per sheet atom it is comparable to graphite (1090 GPa).

We assumed above that the K intercalate between tubes (endo K), but it is possible that the tubes have defects or open ends that allow K to penetrate the tubes. First we calculated the case in which only endo K are allowed. This leads to energetics as in Fig. 1 with an optimum packing of $K_4^{endo}C_{80}$. The structure is in Fig. 2(e) and the powder diffraction pattern is shown in Fig. 4(e). Allowing both endo and exo K, we find an optimum structure of $K_5^{exo}K_3^{endo}C_{80} = KC_{30}$, shown in Figs. 2(f) and 3(b). The powder pattern is in Fig. 4(f).

These calculations suggest a number of experiments to test the predictions and suggest that theory might be used to explore the structures and properties for new compositions in advance of experiment. To help in such analyses, we will make Cerius[2] files of all structures accessible on the Internet [11].

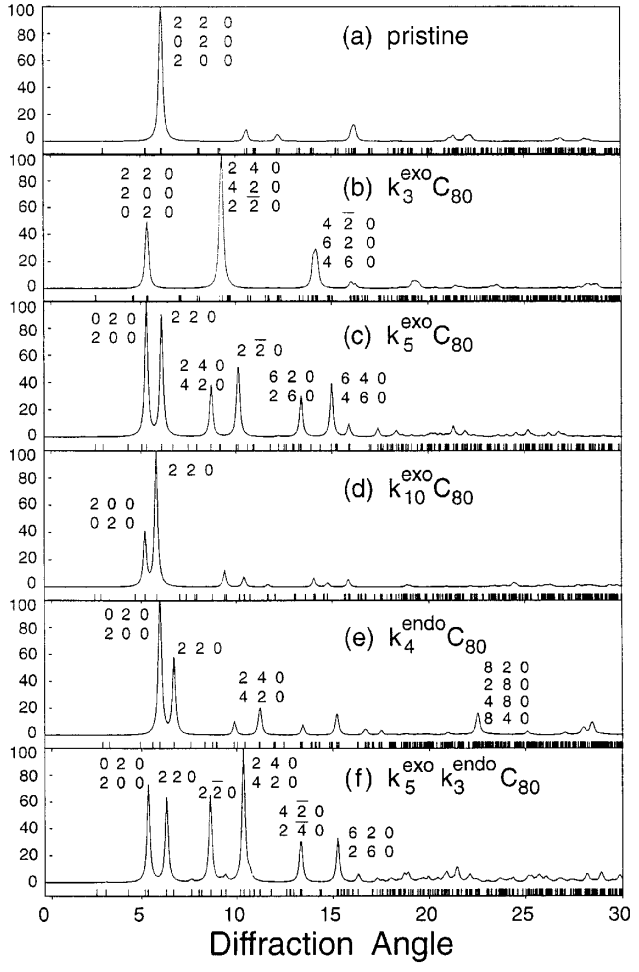

FIG. 4. The powder diffraction patterns for various SWNT/K. The indexing assumes four tubes per unit cell. The intensity is normalized to 100% for the strongest line. These calculations used the Cerius[2] powder diffraction module from Molecular Simulation Inc., San Diego, California.

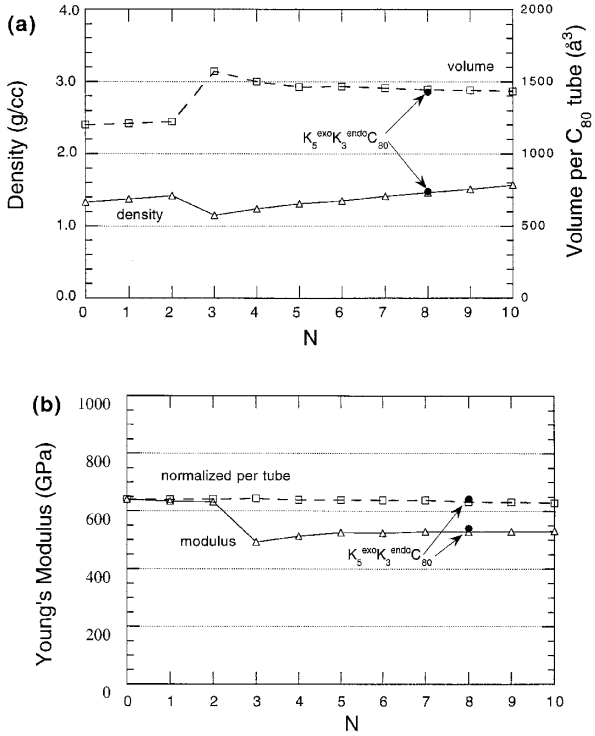

FIG. 5. The density and volume (a) and Young's modulus (b) along the tube axis as a function for n (for trigonal structures and exo K).

This research was funded by NASA (computational nanotechnology) and by NSF-GCAG (ASC 92-100368). The facilities of the MSC are also supported by grants from BP Chemical, Chevron Petroleum Technology, Aramco, Exxon, Owens-Corning, Chevron Chemical Co., Asahi Glass, Chevron Research and Technology Co., Hercules, Avery Dennison, and Beckman Institute. We thank Rick Smalley for an advance copy of Refs. [4] and [5].

*To whom correspondence should be addressed.
Electronic address: wag@wag.caltech.edu

[1] A. Thess, R. Lee, P. Nikolaev, H. Dai, P. Petit, J. Robert, C. Xu, Y. H. Lee, S. G. Kim, A. G. Rinzler, D. T. Colbert, G. E. Scuseria, D. Tomanek, J. E. Fisher, and R. E. Smalley, Science **273**, 183 (1996).

[2] D. S. Bethune, C. H. Kiang, M. S. Devries, G. Gorman, G. R. Savoy, J. Vazquez, and R. Beyers, Nature (London) **363**, 605 (1993); C. H. Kiang and W. A. Goddard III, Phys. Rev. Lett. **76**, 2515 (1996).

[3] S. Iijima and T. Ichlhashi, Nature (London) **363**, 603 (1993).

[4] R. S. Lee, H. J. Kim, J. E. Fischer, A. Thess, and R. E. Smalley, Nature (London) **388**, 255 (1997).

[5] A. M. Rao, P. C. Eklund, S. Bandow, A. Thess, and R. E. Smalley, Nature (London) **388**, 257 (1997).

[6] Y. Guo, N. Karasawa, and W. A. Goddard III, Nature (London) **351**, 464 (1991); G. Chen, Y. Guo, N. Karasawa, and W. A. Goddard III, Phys. Rev. B **48**, 13 959 (1993).

[7] A. Mansour, S. E. Shnatterly, and J. J. Risko, Phys. Rev. Lett. **58**, 614 (1987).

[8] M. S. Dresselhaus and G. Dresselhaus, Adv. Phys. **30**, 139 (1981).

[9] K. T. Lim, S. Burnett, M. Iotov, R. B. McClurg, N. Vaidehi, S. Dasgupta, S. Taylor, and W. A. Goddard III, J. Comput. Chem. **18**, 501 (1997).

[10] A. H. Chang, W. C. Ermler, and R. M. Pitzer, J. Phys. Chem. **95**, 9288 (1991).

[11] Available on the Internet (http://www.wag.caltech.edu/).